BIOLOGY OF REPRODUCTION **74,** 751–759 (2006)
Published online before print 28 December 2005.
DOI 10.1095/biolreprod.105.049254

Deficiency of SPAG16L Causes Male Infertility Associated with Impaired Sperm Motility[1]

Zhibing Zhang,[3] Igor Kostetskii,[3] Waixing Tang,[4] Lisa Haig-Ladewig,[3] Rossana Sapiro,[5] Zhangyong Wei,[4] Aatish M. Patel,[4] Jean Bennett,[4] George L. Gerton,[3] Stuart B. Moss,[3] Glenn L. Radice,[3] and Jerome F. Strauss III[2,6]

Center for Research on Reproduction and Women's Health,[3] and Department of Ophthalmology,[4] University of Pennsylvania Medical Center, Philadelphia, Pennsylvania, 19104
Department of Histology and Embryology,[5] University of the Republic, CP 11800 Montevideo, Uruguay
Department of Obstetrics and Gynecology,[6] Virginia Commonwealth University, Richmond, Virginia, 23298

ABSTRACT

The axonemes of cilia and flagella contain a "9+2" structure of microtubules and associated proteins. Proteins associated with the central doublet pair have been identified in *Chlamydomonas* that result in motility defects when mutated. The murine orthologue of the *Chlamydomonas* PF20 gene, sperm-associated antigen 16 (*Spag16*), encodes two proteins of M_r ~71 × 10^3 (SPAG16L) and M_r ~35 × 10^3 (SPAG16S). In sperm, SPAG16L is found in the central apparatus of the axoneme. To determine the function of SPAG16L, gene targeting was used to generate mice lacking this protein but still expressing SPAG16S. Mutant animals were viable and showed no evidence of hydrocephalus, lateralization defects, sinusitis, bronchial infection, or cystic kidneys—symptoms typically associated with ciliary defects. However, males were infertile with a lower than normal sperm count. The sperm had marked motility defects, even though ultrastructural abnormalities of the axoneme were not evident. In addition, the testes of some nullizygous animals showed a spermatogenetic defect, which consisted of degenerated germ cells in the seminiferous tubules. We conclude that SPAG16L is essential for sperm flagellar function. The sperm defect is consistent with the motility phenotype of the *Pf20* mutants of *Chlamydomonas,* but morphologically different in that the mutant algal axoneme lacks the central apparatus.

gamete biology, sperm, sperm motility and transport, testis

INTRODUCTION

The "9+2" microtubular structure of the axoneme is conserved in most cilia and flagella. The primary role of the nine outer doublet microtubules has been well elucidated, i.e., the associated dynein motors power the microtubule sliding that ultimately results in flagellar bending [1–3]. However, the roles of the radial spokes (RS) and the central pair of microtubules (CP) are not understood well. Much of the current knowledge of CP/RS function is derived from genetic, structural, and functional investigations in *Chlamydomonas*. These studies suggest that the CP/RS serve as mechanochemical sensors to control motility in 9+2 cilia and flagella [4, 5].

A number of central pair proteins have been identified in *Chlamydomonas*. PF6 localizes to the 1a projection on the C1 microtubule. Flagella lacking this protein display a twitching motion [6]. PF16 and PF20 are respectively localized to the C1 microtubule and the intermicrotubule bridge connecting C1 and C2. Mutations in these proteins result in paralyzed flagella with alterations in the organization of the central pair [7, 8]. Other proteins, including PF15, PP1c, KLP1, KRP, AKAP240, and calmodulin, also localize to the CP and its associated structures and have roles in regulating flagella motility [9–14].

Because relatively little is known about the central apparatus in mammalian sperm flagella, we cloned the cDNAs encoding mouse and human SPAG6 and SPAG16 [15–19], orthologues of *Chlamydomonas* PF16 and PF20, respectively, and investigated the functions of these proteins by gene targeting. Within 8 wk of birth, approximately 50% of the SPAG6-deficient mice die from hydrocephalus. Males surviving to maturity are infertile, because their sperm have motility defects and are morphologically abnormal, frequently missing their heads and displaying disorganized axonemal structure [20].

The mouse *Spag16* gene uses alternative promoters to transcribe two major mRNAs (*Spag16_pr1*, 2.5 kb, and *Spag16_pr2*, 1.4 kb), which are differentially expressed during spermatogenesis and encode proteins of M_r ~71 × 10^3 (SPAG16L) and M_r ~35 × 10^3 (SPAG16S), respectively. Both proteins contain contiguous WD repeats in their carboxyl termini, indicative of protein-protein interactions. The meiotically-expressed SPAG16L is found in the cytoplasm of germ cells and then becomes part of the central apparatus of the sperm axoneme. In contrast, the SPAG16S protein is expressed postmeiotically and accumulates in nuclei of spermatids [18, 21]. We previously targeted both the SPAG16L and SPAG16S proteins in embryonic stem (ES) cells by disrupting domains within the *Spag16* gene that encode the WD repeats. Highly chimeric mice carrying the mutant *Spag16* allele have impaired spermatogenesis with a significant loss of germ cells at the round spermatid stage. In addition, a striking disorganization of the sperm axonemal structure is found. The mutated *Spag16* allele is never transmitted, indicating that *Spag16* haploinsufficiency caused the spermatogenetic defects. These findings reveal essential roles for the *Spag16* gene during mouse spermatogenesis: germ cell viability and the integrity of the axoneme [21].

[1]Supported by National Institutes of Health grants HD37416, HD06724, and TW06223–01, and the Foundation Fighting Blindness (FFB).
[2]Correspondence: Jerome F. Strauss, III, School of Medicine, Virginia Commonwealth University, Sanger Hall, 1101 East Marshall Street, Room 1–071, P.O. Box 980565, Richmond, VA 23298.
FAX: 804 828 7628; e-mail: jfstrauss@vcu.edu

Received: 15 November 2005.
First decision: 1 December 2005.
Accepted: 22 December 2005.

ISSN: 0006-3363. http://www.biolreprod.org

The different patterns of expression and localization of SPAG16L and SPAG16S, coupled with the spermatogenic phenotype of the *Spag16*$^{+/-}$ mouse, suggest that these protein variants may have distinct roles during male germ cell development. To study the functions of each protein, we embarked on studies to target the two proteins separately. In the present work, the SPAG16L protein was specifically eliminated by disrupting exons 2 and 3 of *Spag16_pr1*. We found that SPAG16L-deficient male mice were infertile; in particular, their sperm counts were lower than normal, and the sperm had marked motility defects. However, unlike the phenotype of SPAG6-null animals, flagella from SPAG16L-null mouse sperm had no major morphological or ultrastructural defects. Sperm from male mice heterozygous for the targeted mutation of *Spag16_pr1* showed modest but statistically significant motility defects upon computer-assisted motion analysis. The observations suggest that a deficiency in SPAG16L impairs the function of the sperm tail axoneme without causing gross structural changes.

MATERIALS AND METHODS

Targeted Mutation of the Spag16 Gene Region Encoding the SPAG16L Protein

A targeting vector containing a neomycin selection cassette was generated to replace exons 2 and 3 of *Spag16_pr1*. The vector was linearized with *Cla* I and electroporated into TL-1 129/Sv ES cells. ES cell clones that survived G418 selection were evaluated for homologous recombination by Southern blot analysis. Three correctly targeted ES cell clones were used to generate chimeric mice with the assistance of the University of Pennsylvania Medical School Transgenic Mouse Core. These mice were then crossed with C57BL/6J females to obtain heterozygous mutants, and the mouse lines were maintained in on-campus animal facilities. Mice used in these studies were the offspring of crosses between the F_1 and/or F_2 generations (129/Sv/C57BL/6J genetic background). Mice were genotyped by PCR. Two sets of primers were used in the PCR experiments. One set of primers corresponded to the neomycin selection cassette (antisense: 5′-GAACTTCGGAATAGGAACTTC-3′) and *Spag16* gene (sense: 5′-CCATGGTATGGAGATTAGAGGACAACCTC-3′). The other set of primers corresponded to the deleted region of *Spag16_pr1* (sense: 5′-GGTCACCATAACGGAAACATC-3′; antisense: 5′-CAGGAG-CATGTTTTGCAGAGC-3′). The mutated gene is officially designated as the *Spag16*^{tm2Jfs} allele. For simplicity and to designate the specific elimination of the expression of SPAG16L while maintaining expression of SPAG16S, this allele will be referred to as *Spag16_pr1*$^{-}$ throughout this report.

Assessment of Fertility and Fecundity

To assess fertility and fecundity, littermate males (5–7 mo old) of different genotypes (*Spag16_pr1*$^{+/+}$, *Spag16_pr1*$^{+/-}$, and *Spag16_pr1*$^{-/-}$) were each placed in cages with two mature wild-type females for at least 2 mo. Littermate females of different genotypes were each caged with a wild-type fertile male for a similar period of time. The number of mice achieving a pregnancy and the number of offspring from each mating set or pregnancy were recorded.

Northern and Southern Blot Analysis

Northern blots containing total testicular RNA (30 μg/lane) were probed with a full-length *Spag16_pr1* cDNA. Blots were stripped and reprobed for mouse *Akap4* [22], *Spag6*, and *Pf6*. For Southern blotting, ES cell DNA (15 μg/lane) was digested with *Kpn* I and separated on a 0.8% agarose gel. The DNA was transferred to nylon membranes and probed with a *Spag16*-specific probe downstream of the homologous recombination region.

Immunoblot Analysis and Generation of an Anti-SPAG6 Antibody

Equal amounts of testicular or sperm protein (40 μg/lane) were prepared and subjected to immunoblot analysis using antibodies against SPAG6, PF6, AKAP4, and the N- and C-termini of SPAG16 [15–19, 22]. A cDNA encoding the C-terminus (amino acids 250–507) of mouse SPAG6 was cloned in frame into the pET28a vector. The fusion protein was purified and rabbit polyclonal antibodies were generated as reported previously [18].

Motility Assays

Sperm were collected after swimming out from the caudae epididymides into modified Whitten's medium (15 mM Hepes-sodium salt, 1.2 mM $MgCl_2$, 100 mM NaCl, 4.7 mM KCl, 1 mM pyruvic acid, and 4.8 mM lactic acid) for 10 min at 37°C. The solution had a final pH of 7.35. Sperm were counted and diluted to 2×10^6 sperm/ml, and motility was analyzed in a 100-μm chamber (Cell Vision-USA) using the IVOS Sperm Analyzer (Hamilton-Thorne Research). The parameters that were used for the analysis setup are described in the technical guide for the IVOS system, version 12.2 (mouse setup 1). Sperm populations were analyzed as soon as possible after their release from the epididymides. For each sperm sample, a total of 10 fields were analyzed.

Histology, Immunochemistry Microscopy, and Transmission Electron Microscopy

Cauda epididymal sperm, testis, tracheal tissue, kidney, and ependymal tissue were prepared for light and transmission electron microscopy using standard methods, as previously described. Immunochemistry on testes and sperm were performed as previously described [21]. The same mice that were used to assess fertility were used for histological analysis of the testis.

Measurement of Serum Hormone Levels

Testosterone was quantified using a radioimmunoassay kit (TKTT1; Diagnostic Products Corp). FSH and LH were measured by the University of Virginia Center for Research in Reproduction Ligand Assay and Analysis Core (U54-HD28934).

Ethics

Procedures involving animals were conducted under the approval of the Institutional Animal Care and Use Committee of the University of Pennsylvania in accordance with the Guide for Care and Use of Laboratory Animals (Protocol #4365–01).

RESULTS

Targeted Disruption of Spag16_pr1 Eliminates SPAG16L in Germ Cells and Sperm

We disrupted the *Spag16_pr1* gene in murine ES cells by replacing the second and third exons with the *Neo*-resistance gene (Fig. 1A). This manipulation prevented expression of the M_r $\sim 71 \times 10^3$ SPAG16L protein, but allowed expression of the M_r $\sim 35 \times 10^3$ SPAG16S protein. To generate chimeric mice, ES cells carrying the targeted allele of the *Spag16* gene (*Spag16_pr1*$^{-}$; Fig. 1B) were injected into blastocysts which were transferred into pseudopregnant mice. Mutant mice were produced from the chimeric offspring. Disruption of the *Spag16_pr1* genomic region was confirmed by PCR analysis (Fig. 1C) and Southern blotting (data not shown). The proportion of wild-type (37 of 139; 27%), heterozygous (72 of 139; 51%), and nullizygous (30 of 139; 22%) offspring from mating of heterozygous males and females was not significantly different from the expected Mendelian pattern of inheritance (Hardy-Weinberg equilibrium test, Pearson chi square [1] = 0.207, Pr = 0.649). *Spag16_pr1*$^{-/-}$ mice were viable and showed no gross abnormalities. The mutant mice did not display abnormalities in non-reproductive tract tissues (e.g., polycystic kidneys) nor were there laterality defects (situs inversus)—abnormalities associated with defects in ciliogenesis and immotile cilia syndrome [23, 24]. Hydrocephalus was not found in the analysis of brains from 10 mutant mice.

The absences of the 2.5 kb *Spag16_pr1* mRNA and its corresponding M_r $\sim 71 \times 10^3$ SPAG16L protein in the testes of *Spag16_pr1*$^{-/-}$ mice were confirmed by both Northern and

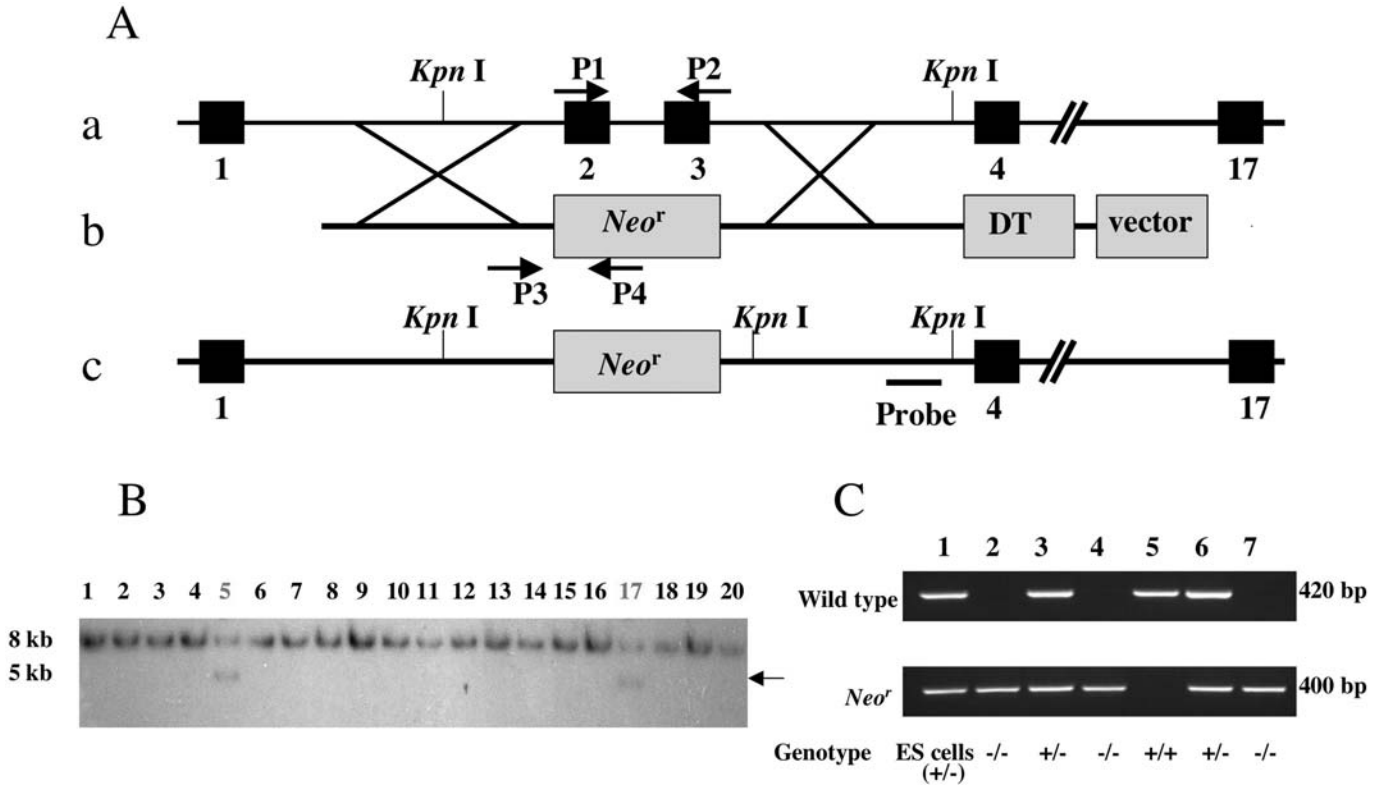

FIG. 1. Targeted disruption of mouse *Spag16_pr1* expression. **A**) Schematic representation of the strategy used to disrupt *Spag16_pr1*. **a**) Partial genomic structure of the *Spag16* gene. **b**) Map of the targeting vector. **c**) Map of the mutated allele. K, *Kpn* I; *Neo*^{r}, neomycin resistance gene; DT, diphtheria toxin; P1 and P2, primers for amplifying the wild-type allele; P3 and P4, primers for amplifying the mutant allele. **B**) Southern blot analysis of transfected embryonic cell clones. An external probe gave rise to a single 8-kb band in wild-type genomic DNA digested with *Kpn* I and a 5-kb band in the mutant DNA (arrow). **C**) Genotyping for wild-type (+) and targeted null (–) alleles of *Spag16_pr1* by PCR. The wild-type allele yielded a 420-bp amplicon that is absent in the homozygous mutant. The smaller 400-bp amplicon representing the *Neo* cassette was detectable only when a targeted allele was present.

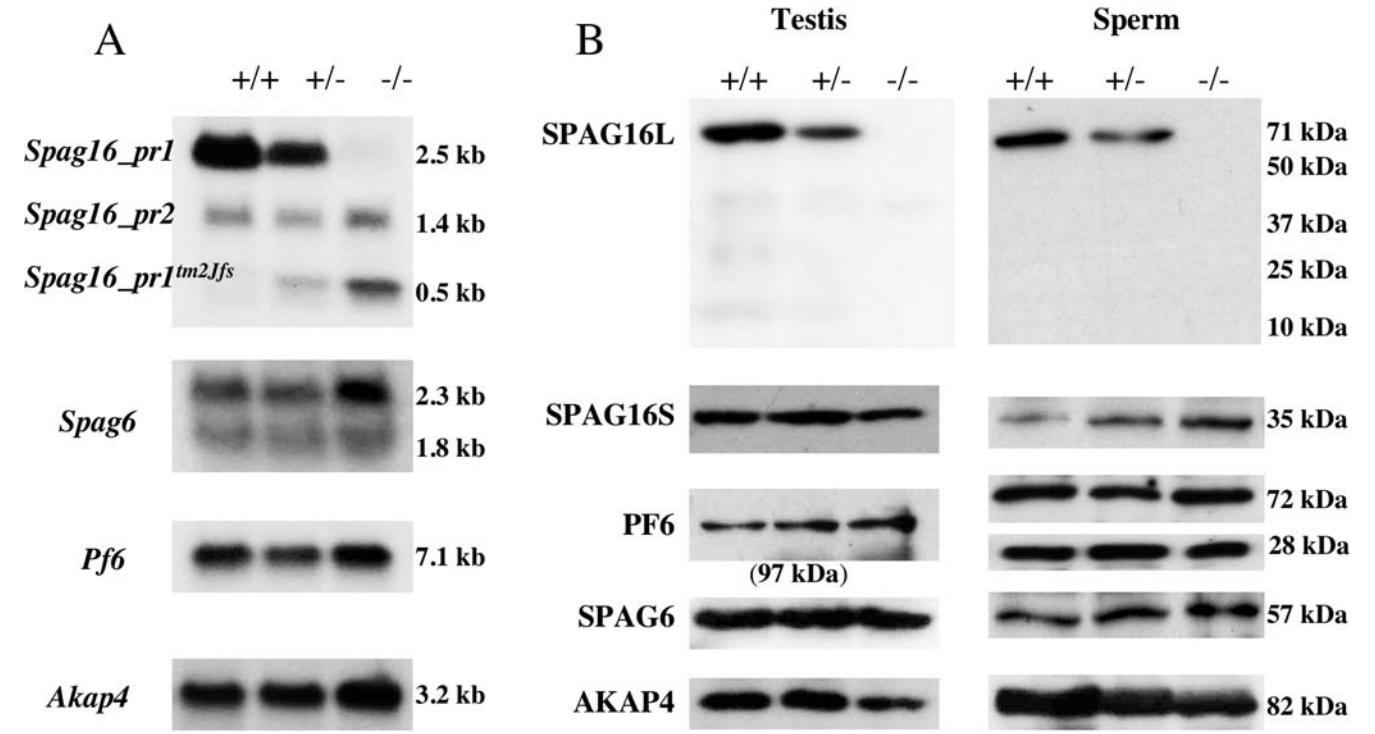

FIG. 2. *Spag16_pr1* mRNA and SPAG16L protein are not present in testis and sperm from null animals. **A**) Northern blot analysis of testicular mRNA expression from *Spag16_pr1*$^{+/+}$ (+/+), *Spag16_pr1*$^{+/-}$ (+/–), and *Spag16_pr1*$^{-/-}$ (–/–) animals. *Spag16_pr1*^{tm2Jfs} refers to the mRNA expressed from the mutant allele. **B**) Immunoblot blot analysis of testicular and sperm protein from *Spag16_pr1*$^{+/+}$ (+/+), *Spag16_pr1*$^{+/-}$ (+/–), and *Spag16_pr1*$^{-/-}$ (–/–) animals.

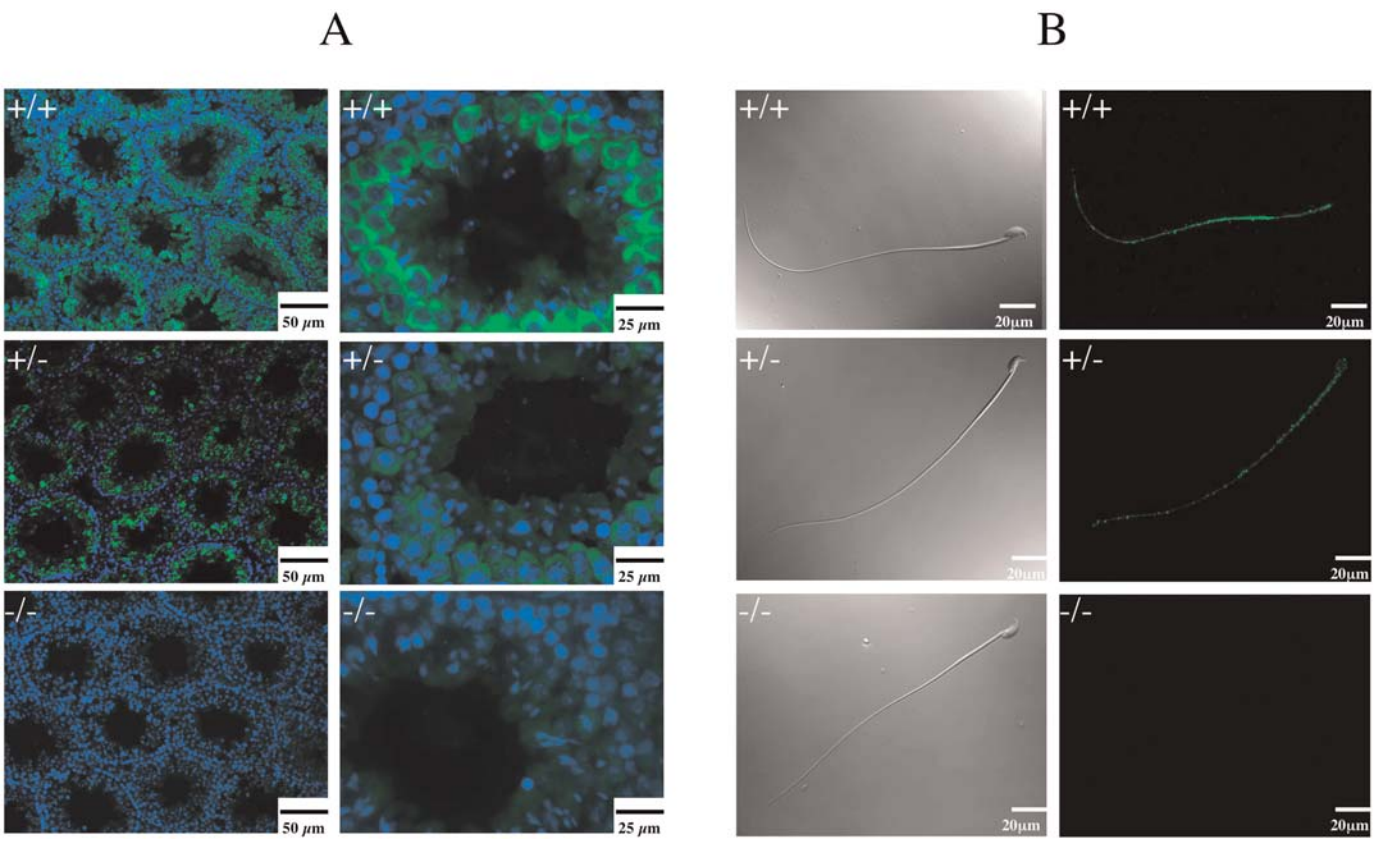

FIG. 3. SPAG16L is localized to the cytoplasm of germ cells and to the axoneme of wild-type sperm. **A**) Immunostaining of SPAG16L in testes from *Spag16_pr1*$^{+/+}$ (+/+), *Spag16_pr1*$^{+/-}$ (+/–), and *Spag16_pr*$^{-/-}$ (–/–) animals. The intensely stained cells are pachytene spermatocytes. **B**) Immunostaining of SPAG16L in Triton X-100-permeabilized sperm from *Spag16_pr1*$^{+/+}$ (+/+), *Spag16_pr1*$^{+/-}$ (+/–), and *Spag16_pr1*$^{-/-}$ (–/–) animals.

immunoblot analyses (Fig. 2, A and B). Although a truncated 0.5 kb mRNA was found in the testes of heterozygous and null animals, a truncated protein corresponding to SPAG16L was not detectable. As might be expected, both the 1.4 kb *Spag16_pr2* mRNA and the encoded $M_r \sim 35 \times 10^3$ SPAG16S protein were present in normal amounts in testicular cells. The mRNA and protein levels of other central pair proteins, e.g., PF6 and SPAG6, did not change in testes and sperm of null animals when compared to their wild-type littermates (Fig. 2, A and B). In addition, the testes of *Spag16_pr1*$^{-/-}$ mice contained *Akap4* mRNA and its encoded protein, AKAP4, the major fibrous sheath component of the sperm flagellum (Fig. 2, A and B).

An antibody that specifically recognizes SPAG16L, but not SPAG16S, showed that the protein is expressed in the cytoplasm of germ cells and along the entire length of the flagella of epididymal sperm in wild-type animals (Fig. 3, A and B). Similar but less robust staining patterns were seen in the testis and sperm of heterozygous animals. No detectable staining was observed in germ cells and sperm of null mice.

SPAG16L is Required for Male but Not Female Fertility

Spag16_pr1$^{-/-}$ males that were mated with wild-type females produced no pregnancies after more than 2 mo of continuous cohabitation even though vaginal plugs were observed in the females (Table 1). The *Spag16_pr1*$^{+/-}$ littermates were all fertile, producing as many offspring per pregnancy as wild-type littermates. All 6 *Spag16_pr1*$^{-/-}$ females achieved a pregnancy during the observation period, and the time to establish a pregnancy was the same as that of wild-type and heterozygous littermates.

Spermatogenic Defects Are Present in Some Spag16_pr1$^{-/-}$ *Mice*

Testicular histology of *Spag16_pr1*$^{+/+}$ and *Spag16_pr1*$^{+/-}$ mice showed that a normal structure of the seminiferous tubules was present (Fig. 4, A–D). Although the testes from three *Spag16_pr1*$^{-/-}$ mice also were normal (Fig. 4, E and F), three other mice of the same genotype from two different ES clones showed abnormalities in spermatogenesis at the round spermatid stage; degenerated germ cells were seen (Fig. 4, G and H). Two of these animals from the same ES clone also had smaller testes (about two thirds and one half normal size). Although a general trend toward a smaller size was observed, the weights of testes and seminal vesicles of *Spag16_pr1*$^{-/-}$ males were not statistically different from those of their wild-type littermates. Serum testosterone, FSH, and LH levels were

TABLE 1. Fertility and fecundity of *Spag16_pr1* mice caged with wild-type C57BL/6J mice of the opposite sex for 2 mo or more.

Spag16_pr1 genotype	Male fertility[a]	Litter size	Female fertility[a]	Litter size
+/+	8/8	8.2 ± 0.4	8/8	7.9 ± 0.6
+/–	8/8	7.9 ± 0.5	8/8	8.1 ± 0.6
–/–	0/9	0	6/6	7.4 ± 0.5

[a]Number of fertile mice/total number of mice.

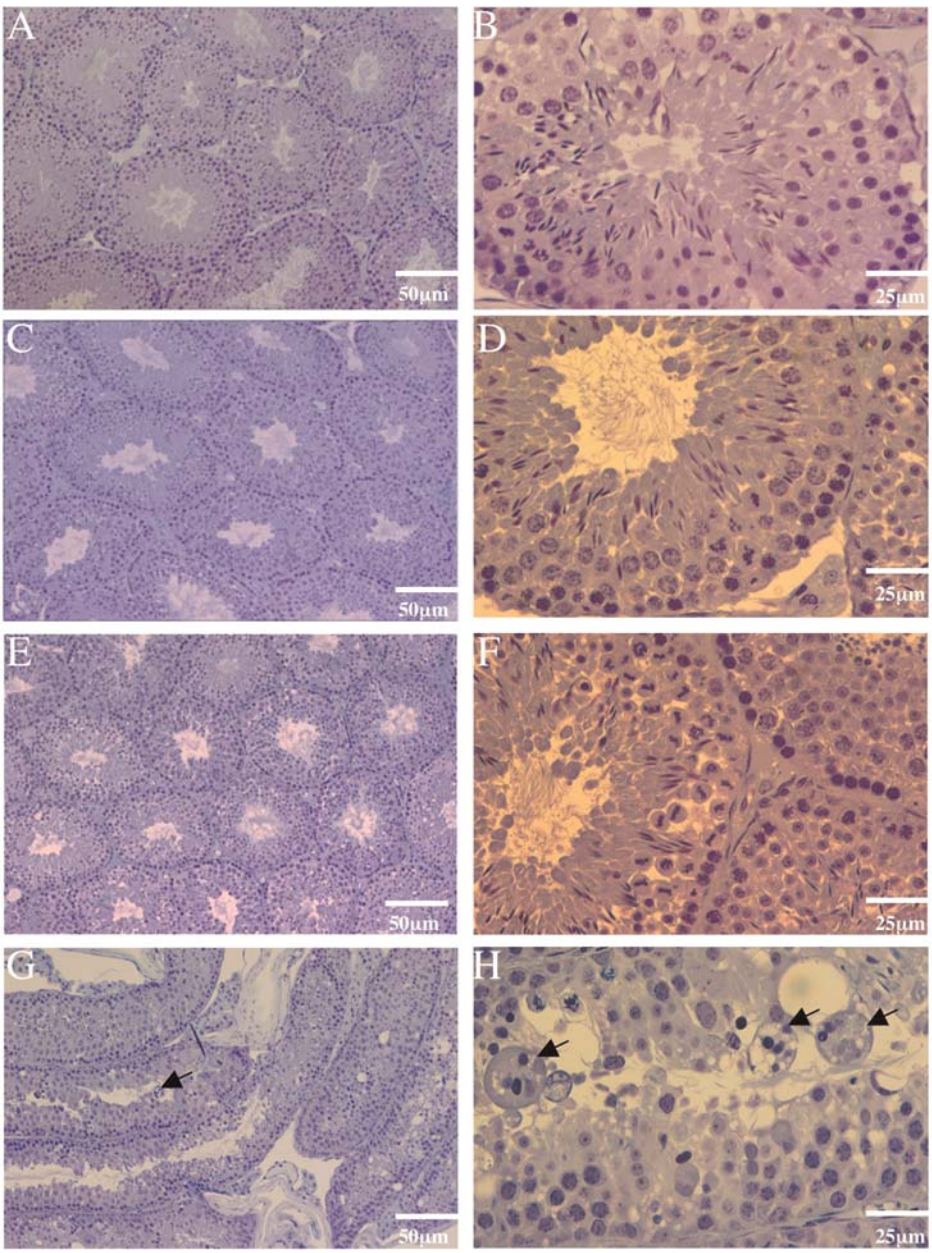

FIG. 4. Testes from some *Spag16_pr1*$^{-/-}$ animals show a mild spermatogenic defect. **A**, **B**) Histology of a *Spag16_pr1*$^{+/+}$ testis. **C**, **D**) Histology of a *Spag16_pr1*$^{+/-}$ testis. **E**, **F**) Histology of a normal *Spag16_pr1*$^{-/-}$ testis. **G**, **H**). Histology of an abnormal *Spag16_pr1*$^{-/-}$ testis; arrows indicate degenerating germ cells. The testicular defects observed are focal. Original magnification **A**, **C**, **E**, and **G** ×100; **B**, **D**, **F**, and **H** ×400.

TABLE 2. Testis and seminal vesicle weights and serum hormone levels.

Genotype	Testis/body weight (mg/g)[a,b]	Seminal vesicle/body weight (mg/g)[a,b]	Testosterone (ng/dl)[a,b]	LH (ng/ml)[a,b]	FSH (ng/ml)[a,b]
Spag16_pr1$^{+/+}$	8.05 ± 0.42 [n = 9]	6.40 ± 0.50 [n = 9]	455.4 ± 108.9 (14.5–888) [n = 9]	0.63 ± 0.08 (0.3–1.08) [n = 9]	35.29 ± 6.63 (18.48–63.5) [n = 6]
Spag16_pr1$^{+/-}$	8.03 ± 0.48 [n = 9]	6.09 ± 0.47 [n = 9]	201.0 ± 77.6 (9.8–625) [n = 8]	0.93 ± 0.24 (0.133–2.326) [n = 8]	30.57 ± 5.41 (18.51–49.72) [n = 5]
Spag16_pr1$^{-/-}$	7.10 ± 0.77 [n = 9]	5.70 ± 0.42 [n = 9]	184.1 ± 82.8 (10.6–702.6) [n = 9]	0.56 ± 0.11 (0.26–1.40) [n = 9]	27.70 ± 3.76 (13.18–45.76) [n = 8]

[a]Values are means ± SEM, $P > 0.05$.
[b]Ranges of mice analyzed are listed in parentheses; numbers of mice analyzed are listed in brackets.

TABLE 3. Sperm motility characteristics.

Spag16_pr1 genotype	n[a]	Sperm concentration (10^6/ml)[b]	Motile sperm (%)[b]	Progressive sperm (%)[b]	Curvilinear velocity[b]	Linearity[b]
+/+	7	28.43 ± 4.11	69.29 ± 4.58	69.00 ± 4.72	255.5 ± 6.99	36.43 ± 1.11
+/–	8	27.47 ± 3.18	55.50 ± 4.57*	55.25 ± 4.66*	225.5 ± 10.60	39.38 ± 1.80
–/–	8	13.93 ± 2.77**	25.63 ± 7.92**	25.50 ± 7.94**	132.5 ± 8.38**	34.13 ± 1.58

[a] Number of males tested.
[b] Values are means ± SEM; *$P < 0.05$ compared to wild-type, **$P < 0.001$ compared to wild-type.

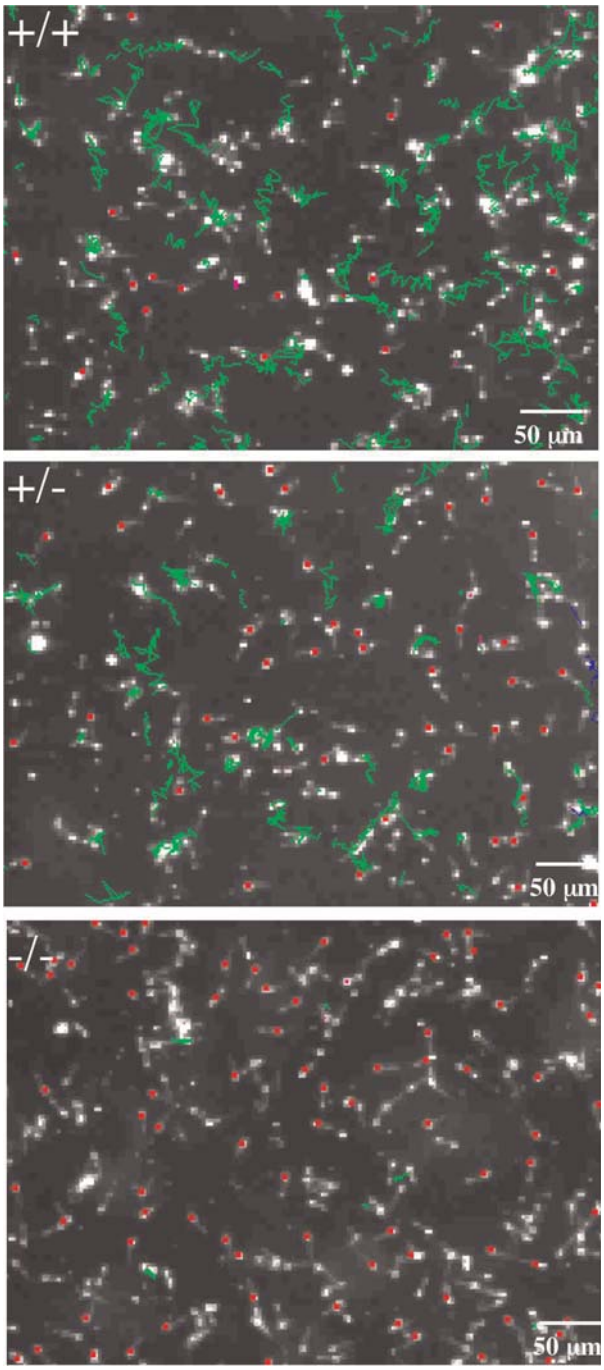

FIG. 5. Sperm motility from *Spag16_pr1*$^{-/-}$ animals is aberrant. Representative tracks of sperm motion from *Spag16_pr1*$^{+/+}$ (+/+), *Spag16_pr1*$^{+/-}$ (+/–), and *Spag16_pr1*$^{-/-}$ (–/–) animals were analyzed by CASA. Sperm from wild-type and heterozygous animals each showed long forward progressive tracks, but sperm from a null animal showed a shorter and aberrant movement.

also examined in several animals of each genotype but were not found to vary in a meaningful way (Table 2).

SPAG16L-Deficient Sperm Have Motility Defects

Sperm were present in the testes and efferent ducts of null animals; however, the numbers of sperm recovered from the caudae epididymides were significantly lower when compared to wild-type males (Table 3). In addition, computer-assisted sperm analysis demonstrated that sperm motility differed between wild-type and mutant animals. Whereas wild-type sperm displayed vigorous flagellar activity and progressive long track forward movement, only a small percentage of the *Spag16_pr1*$^{-/-}$ epididymal sperm were motile and showed progressive forward motility (Table 3, Figs. 5 and 6, and Supplemental Movie available online at http://www.biolreprod.org). Generally, flagellar movement was limited to a slow, erratic waveform with a very low amplitude. In addition, the mean curvilinear velocity (VCL) of motile sperm, an estimate of instantaneous sperm swimming speed, was significantly less in *Spag16_pr1*$^{-/-}$ mice. Interestingly, sperm from *Spag16_pr1*$^{+/-}$ mice had an intermediate VCL value, suggesting that, although these animals were fertile, the inactivation of one *Spag16_pr1* allele impairs flagellar activity because of a reduction in SPAG16L protein (Figs. 2B and 3B). There were no differences in linearity of motile sperm, an estimate of the straightness of the sperm track, between wild-type and mutant sperm (Table 3).

Despite these motility defects, light microscopic examination revealed that more than 99% of the epididymal sperm from *Spag16_pr1*$^{-/-}$ animals were morphologically normal. Heads were not detached from the tails, something that was common in sperm from SPAG6-deficient mice, and no obvious disorganization of the axoneme was observed. Further, transmission electron microscopic analysis of testicular and epididymal sperm revealed that *Spag16_pr1*$^{-/-}$ testes and sperm had a normal axonemal structure (Fig. 7 and Table 4). In particular, the central pair of microtubules was present.

DISCUSSION

Both the mouse *Spag16* and human *SPAG16* genes encode two proteins of $M_r \sim 71 \times 10^3$ (SPAG16L) and $M_r \sim 35 \times 10^3$ (SPAG16S), which have different locations in male germ cells and sperm. SPAG16L is found initially in the cytoplasm of germ cells and then in the central apparatus of the sperm axoneme, whereas SPAG16S is present in nuclei of germ cells. Previously, a targeted deletion that eliminated both proteins resulted in impaired spermatogenesis and a disorganized sperm axoneme in chimeric mice [21]. The inability of the chimeric mice to transmit the mutant *Spag16* allele, presumably because of haploinsufficiency, suggested that the gene has an important role during spermatogenesis. However, this approach did not allow the individual functions of SPAG16L and SPAG16S to be ascertained.

To study the function of SPAG16L, we deleted exons that were not present in the SPAG16S protein by gene targeting.

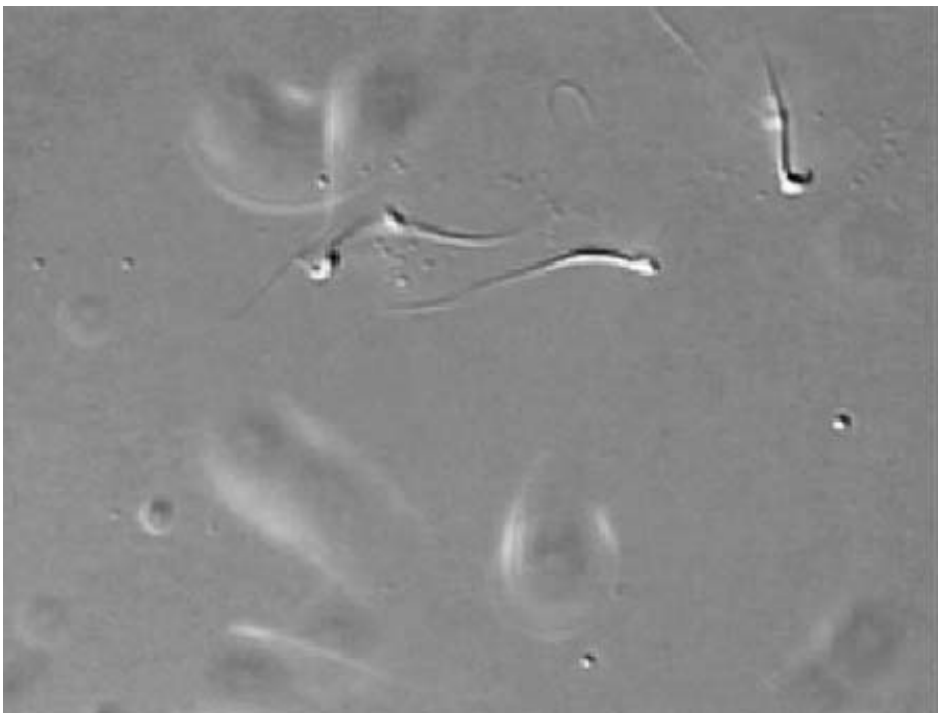

FIG. 6. Examples of sperm motility patterns from the *Spag16_pr1* mutants (see Supplemental Movie available online at http://www.biolreprod.org).

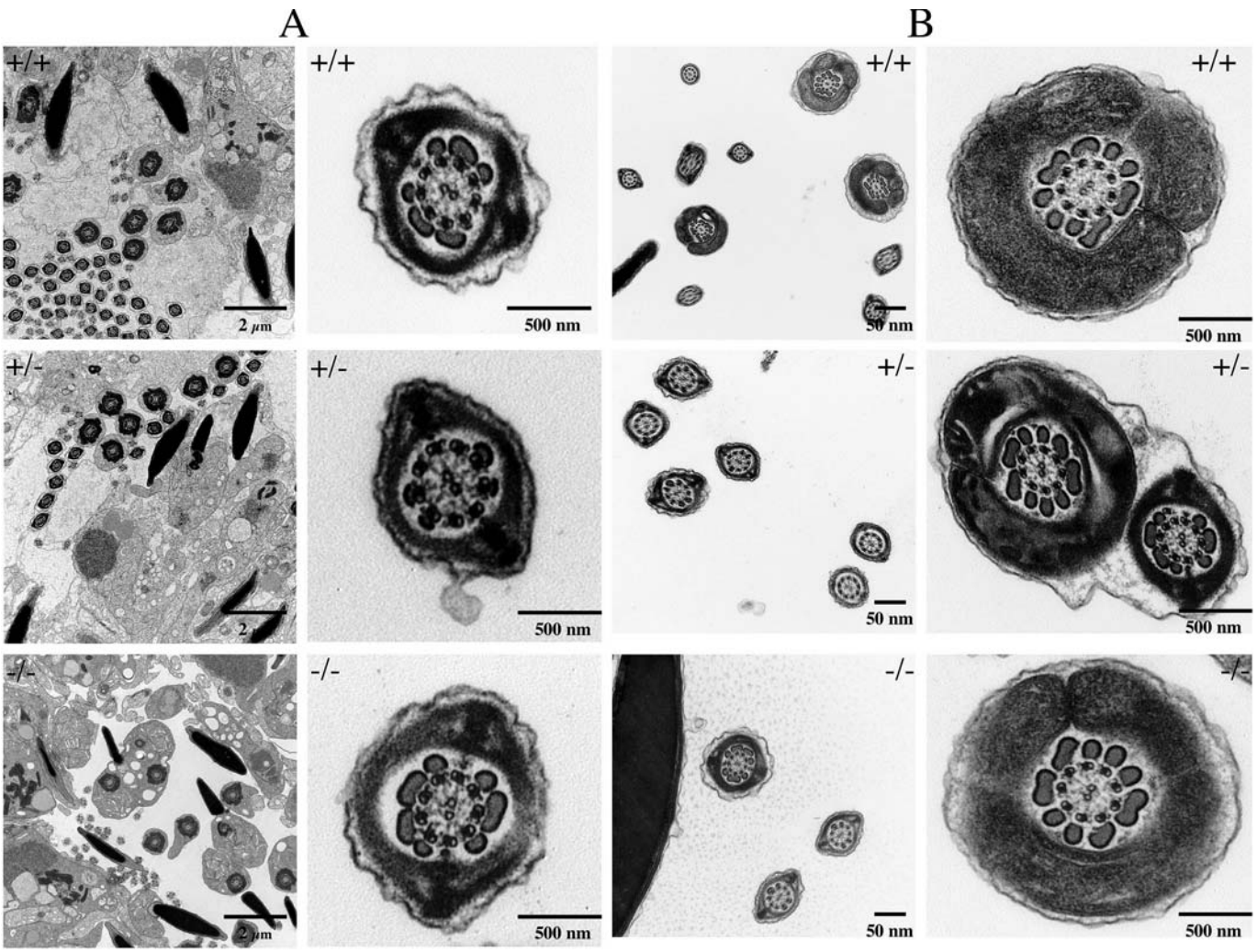

FIG. 7. Ultrastructure of testicular and epididymal sperm. **A**) Testicular sperm from *Spag16_pr1*$^{+/+}$ (+/+), *Spag16_pr1*$^{+/-}$ (+/–), and *Spag16_pr1*$^{-/-}$ (–/–) animals. **B**) Epididymal sperm from *Spag16_pr1*$^{+/+}$ (+/+), *Spag16_pr1*$^{+/-}$ (+/–), and *Spag16_pr1*$^{-/-}$ (–/–) animals.

TABLE 4. Ultrastructural analysis of sperm by transmission electron microscopy.[a]

Region[b]	Normal flagella (%)[c]			Flagella with abnormal outer doublet microtubules (%)[c]		
	+/+	+/–	–/–	+/+	+/–	–/–
Epididymal sperm						
MP	100	100	100	0	0	0
PP	100	99.2 ± 2	100	0	0	0.8 ± 0.4
Testicular sperm						
MP	100	98.4 ± 1.3	100	0	1.6 ± 0.3	0
PP	100	100	100	0	0	0

[a]Sperm from wild-type (+/+), *Spag16_pr1*$^{+/-}$ (+/–), and *Spag16_pr1*$^{-/-}$ (–/–) mice (three for each genotype) were examined by transmission electron microscopy. A total of 135 wild-type, 126 heterozygous, and 112 homozygous mutant epididymal sperm and 151 wild-type, 120 heterozygous, and 108 homozygous mutant testicular sperm were examined.
[b]MP, midpiece; PP, principal piece.
[c]Values are means ± SEM.

Unlike the targeted deletion of both SPAG16L and SPAG16S, chimeric mice were able to transmit the mutant *Spag16_pr1*$^{-}$ allele. The resulting null mice were viable even though they did not express SPAG16L. These animals showed no evidence of hydrocephalus, lateralization defects, sinusitis, bronchial infection or cystic kidneys—conditions typically associated with ciliary defects. However, males were infertile; although some mice had a mild spermatogenetic defect, others did not. In general, these animals had significantly lower sperm counts compared to their wild-type littermates. Most striking, sperm from *Spag16_pr1*$^{-/-}$ animals had marked motility defects, even though the axonemal structure was normal at the ultrastructural level. The absence of a severe spermatogenic defect in this SPAG16L mouse model indicates that it is SPAG16S that causes the serious deficiency in spermatogenesis seen in males in which both SPAG16L and SPAG16S were eliminated. SPAG16S is related to a *Drosophila* testis-specific transcription factor, Cannonball [25], raising the possibility that it has an essential role in mouse spermatogenesis. In contrast, SPAG16L has a different function from SPAG16S, in that it appears to play an important role in sperm motility.

Although both the murine SPAG16L and the *Chlamydomonas* PF20 proteins are critical for flagellar motility, distinctly different phenotypes are observed when the two proteins were mutated/eliminated. When *Chlamydomonas* PF20 is mutated, flagella become paralyzed and the axoneme lacks its entire central apparatus [8]. In contrast, sperm from *Spag16_pr1*$^{-/-}$ mice showed a very shallow beat with little bend formation, suggesting a defect in the attachment of the spoke heads to the central pair apparatus or a deformation of this structure [26]. In addition, these sperm had no obvious structural defects in the axoneme, i.e., the central pair was present. The differences between these two phenotypes suggest a number of possibilities. The locations of the proteins in the central pair may differ. Although PF20 is localized to the bridge connecting C1 and C2 in the central apparatus in *Chlamydomonas*, it is not known whether SPAG16L which by immunoelectron microscopy is localized on or around the central apparatus, shares an identical position in the bridge connecting the two central microtubules. In addition, the presence of WD repeats suggests that SPAG16L interacts with other central pair proteins. Such a protein complex may be more stable in the absence of SPAG16 in the axoneme of the mouse compared to *Chlamydomonas* because of differences in the composition of the interacting proteins.

The phenotype of the SPAG16L-null mouse also is different from mice in which another central pair protein, SPAG6, has been targeted. SPAG6-null animals have a more severe phenotype as it affects the axonemal structure in both cilia and flagella of males and females. These mice have a lower body weight, and 50% die from hydrocephalus within 8 wk of age, presumably reflecting abnormalities in the function of cilia of ependymal cells. Unlike the SPAG6 mutant mice, body weight was not affected in the SPAG16L-null mice, and none of the mutant mice developed hydrocephalus. This suggests that SPAG6 has a more important role in maintaining the flagellar structure and function in mammals. Our previous studies indicate that SPAG6 may be the nexus linking SPAG16 and PF6, because in vitro studies showed that SPAG6 recruits both SPAG16L and PF6 to microtubules [17]. Thus, the sperm motility defects in the SPAG16L-deficient mice may reflect a disruption in the functional interactome of central apparatus proteins.

The presence of a mild spermatogenetic defect in SPAG16L-null mice is intriguing. Some, but not all, of these animals had smaller than normal testes and impaired spermatogenesis at the round spermatid stage. In contrast, when both SPAG16L and SPAG16S were eliminated, a severe spermatogenetic defect was evident. Although this suggests that SPAG16S is primarily responsible for the spermatogenetic defect, it is possible that SPAG16L contributes to the phenotype. In this regard, we have found that SPAG16L interacts with the chromosome condensing-like protein (CCLP) in a yeast 2-hybrid assay (unpublished data). Although relatively little is known about CCLP, its message is highly expressed in testis between 20 and 30 days after birth, when the germ cells are undergoing dramatic change, including nucleus condensation [27]. Thus, it is possible that SPAG16L interacts with CCLP to affect events in nuclear remodeling that occur during spermatogenesis.

The male infertility phenotype caused by a marked reduction in sperm motility and the absence of gross abnormalities in tissues containing ciliated cells indicates that SPAG16L could be a good molecular target for male contraception. Hormonal suppression of spermatogenesis by administration of exogenous hormones to interfere with the hypothalamic-pituitary-testicular axis has been the primary approach for male contraception, but concerns about side effects from these endocrine methods are substantial [28]. Nonhormonal approaches that affect only male germ cell function represent a more innovative strategy for the development of novel contraceptives for the male. There are increasing numbers of meiotically and postmeiotically expressed germ-cell-specific gene products involved in different aspects of spermatogenesis and sperm function that theoretically could serve as targets for intervention [29]. Our findings highlight the possibility of a nonhormonal approach for male contraception by the targeting of SPAG16L function.

ACKNOWLEDGMENTS

We thank Jean Richa and Peifu He (Transgenic Core, University of Pennsylvania Medical Center, Philadelphia) for help with injection of the ES cells. Transmission electron microscopy was performed in the Imaging Core of the University of Pennsylvania's Diabetes Center (DK19525). Follicle-stimulating hormone and luteinizing hormone levels were measured at the University of Virginia Center for Research in Reproduction Ligand Assay and Analysis Core (U54-HD28934).

REFERENCES

1. Satir P. Studies on cilia. 3. Further studies on the cilium tip and a "sliding filament" model of ciliary motility. J Cell Biol 1968; 39:77–94.
2. Brokaw CJ. Flagellar movement: a sliding filament model. Science 1972; 178:455–462.
3. Shingyoji C, Murakami A, Takahashi K. Local reactivation of Triton-extracted flagella by iontophoretic application of ATP. Nature 1977; 265: 269–270.
4. Smith EF, Yang P. The radial spokes and central apparatus: mechano-chemical transducers that regulate flagellar motility. Cell Motil Cytoskeleton 2004; 57:8–17.
5. Mitchell DR. Speculations on the evolution of 9+2 organelles and the role of central pair microtubules. Biol Cell 2004; 96:691–696.
6. Rupp G, O'Toole E, Porter ME. The Chlamydomonas PF6 locus encodes a large alanine/proline-rich polypeptide that is required for assembly of a central pair projection and regulates flagellar motility. Mol Biol Cell 2001; 12:739–751.
7. Smith EF, Lefebvre PA. PF16 encodes a protein with armadillo repeats and localizes to a single microtubule of the central apparatus in Chlamydomonas flagella. J Cell Biol 1996; 132:359–370.
8. Smith EF, Lefebvre PA. PF20 gene product contains WD repeats and localizes to the intermicrotubule bridges in Chlamydomonas flagella. Mol Biol Cell 1997; 8:455–467.
9. Dymek EE, Lefebvre PA, Smith EF. PF15p is the chlamydomonas homologue of the Katanin p80 subunit and is required for assembly of flagellar central microtubules. Eukaryot Cell 2004; 3:870–879.
10. Yang P, Diener DR, Rosenbaum JL, Sale WS. Localization of calmodulin and dynein light chain LC8 in flagellar radial spokes. J Cell Biol 2001; 153:1315–1326.
11. Bernstein M, Beech PL, Katz SG, Rosenbaum JL. A new kinesin-like protein (Klp1) localized to a single microtubule of the Chlamydomonas flagellum. J Cell Biol 1994; 125:1313–1326.
12. Gaillard AR, Diener DR, Rosenbaum JL, Sale WS. Flagellar radial spoke protein 3 is an A-kinase anchoring protein (AKAP). J Cell Biol 2001; 153: 443–448.
13. Mitchell DR, Sale WS. Characterization of a Chlamydomonas insertional mutant that disrupts flagellar central pair microtubule-associated structures. J Cell Biol 1999; 144:293–304.
14. Smith EF. Regulation of flagellar dynein by calcium and a role for an axonemal calmodulin and calmodulin-dependent kinase. Mol Biol Cell 2002; 13:3303–3313.
15. Neilson LI, Schneider PA, Van Deerlin PG, Kiriakidou M, Driscoll DA, Pellegrini MC, Millinder S, Yamamoto KK, French CK, Strauss JF 3rd. cDNA cloning and characterization of a human sperm antigen (SPAG6) with homology to the product of the Chlamydomonas PF16 locus. Genomics 1999; 60:272–280.
16. Sapiro R, Tarantino LM, Velazquez F, Kiriakidou M, Hecht NB, Bucan M, Strauss JF 3rd. Sperm antigen 6 is the murine homologue of the Chlamydomonas reinhardtii central apparatus protein encoded by the PF16 locus. Biol Reprod 2000; 62:511–518.
17. Zhang Z, Jones BH, Tang W, Moss SB, Wei Z, Ho C, Pollack M, Horowitz E, Bennett J, Baker ME, Strauss JF 3rd. Dissecting the axoneme interactome: the mammalian orthologue of Chlamydomonas PF6 interacts with sperm-associated antigen 6, the mammalian orthologue of Chlamydomonas PF16. Mol Cell Proteomics 2005; 4:914–923.
18. Zhang Z, Sapiro R, Kapfhamer D, Bucan M, Bray J, Chennathukuzhi V, McNamara P, Curtis A, Zhang M, Blanchette-Mackie EJ, Strauss JF 3rd.. A sperm-associated WD repeat protein orthologous to Chlamydomonas PF20 associates with Spag6, the mammalian orthologue of Chlamydomonas PF16. Mol Cell Biol 2002; 22:7993–8004.
19. Horowitz E, Zhang Z, Jones BH, Moss SB, Ho C, Wood JR, Wang X, Sammel MD, Strauss JF 3rd. Patterns of expression of sperm flagellar genes: early expression of genes encoding axonemal proteins during the spermatogenic cycle and shared features of promoters of genes encoding central apparatus proteins. Mol Hum Reprod 2005; 11:307–317.
20. Sapiro R, Kostetskii I, Olds-Clarke P, Gerton GL, Radice GL, Strauss JF 3rd. Male infertility, impaired sperm motility, and hydrocephalus in mice deficient in sperm-associated antigen 6. Mol Cell Biol 2002; 22:6298–6305.
21. Zhang Z, Kostetskii I, Moss SB, Jones BH, Ho C, Wang H, Kishida T, Gerton GL, Radice GL, Strauss JF 3rd. Haploinsufficiency for the murine orthologue of Chlamydomonas PF20 disrupts spermatogenesis. Proc Natl Acad Sci U S A 2004; 101:12946–12951.
22. Carrera A, Gerton GL, Moss SB. The major fibrous sheath polypeptide of mouse sperm: structural and functional similarities to the A-kinase anchoring proteins. Dev Biol 1994; 165:272–284.
23. Pazour GJ, Dickert BL, Vucica Y, Seeley ES, Rosenbaum JL, Witman GB, Cole DG. Chlamydomonas IFT88 and its mouse homologue, polycystic kidney disease gene tg737, are required for assembly of cilia and flagella. J Cell Biol 2000; 151:709–718.
24. Schneider H, Brueckner M. Of mice and men: dissecting the genetic pathway that controls left-right asymmetry in mice and humans. Am J Med Genet 2000; 97:258–270.
25. Hiller MA, Lin TY, Wood C, Fuller MT. Developmental regulation of transcription by a tissue-specific TAF homolog. Genes Dev 2001; 15: 1021–1030.
26. Lindemann CB. Structural-functional relationships of the dynein, spokes, and central-pair projections predicted from an analysis of the forces acting within a flagellum. Biophys J 2003; 84:4115–4126.
27. Eddy EM. The germ line and development. Dev Genet 1996; 19:287–289.
28. Cornia PB, Anawalt BD. Male hormonal contraception. Expert Opin Emerg Drugs 2004; 9:335–344.
29. Ivell R, Danner S, Fritsch M. Post-meiotic gene products as targets for male contraception. Mol Cell Endocrinol 2004; 216:65–74.